Steel and Composite Structures, *Vol. 57, No. 5 (2025) 459-475*
https://doi.org/10.12989/scs.2025.57.5.459

Optimizing column point brace designs: Balancing strength and stiffness with buckling load equivalence method

Kee Dong Kim[1a], Jeonghwa Lee[*1], Kyoung Yong Park[2a] and Young-Goo Choi[3a]

[1]*Department of Smart Infrastructure Engineering, Kongju National University, Cheonan-si 31080, Republic of Korea*
[2]*Chief Creative Officer, DS Global ECM Co., Ltd., Seoul, Republic of Korea*
[3]*Chief Technology Officer, ANS Co., Ltd., Seoul, Republic of Korea*

(Received June 11, 2025, Revised October 24, 2025, Accepted November 15, 2025)

Abstract. This study explores the potential for using smaller braces by increasing strength requirements and reducing stiffness, thereby challenging traditional stiffness-governed design approaches. The buckling load equivalence method (BEM), which assumes that the buckling load of an imperfect column at infinite lateral displacement equals that of a perfectly straight column, was evaluated alongside the Castigliano model (CM) and the Winter model (WM). For fully braced systems, CM and WM produced nonconservative estimates, while BEM yielded more conservative results than finite element analysis (FEA). In partially braced systems, all three models gave conservative estimates compared to FEA, with CM being the least conservative and WM the most. FEA results showed that bracing forces in full bracing scenarios exceeded 1% of column strength and increased with more braces, even when critical stiffness was doubled. This indicates that stiffness alone does not govern brace force requirements. The study highlights the importance of balanced brace optimization, which emphasizes reduced stiffness and increased strength to achieve more efficient designs. By applying an optimal varying amplification factor, smaller brace sizes can meet strength demands per AISC specifications while remaining below linearized stiffness limits. The proposed BEM approach effectively balances strength, stiffness, and efficiency in brace design.

Keywords: balanced optimal design; bracing force; bracing stiffness; buckling load; multiple-point braces

1. Introduction

As the structural performance and mechanical properties of materials improve, buckling issues may become more significant (Lee 2004, Hawileh *et al*. 2012, Lee *et al*. 2022, Seo *et al*. 2022, Leblouba *et al*. 2024). Since column buckling can lead to catastrophic failure of the entire structural system, it is essential to minimize the likelihood of buckling during the design process. The Intermediate-point braces enhance the resistance of the column to buckling by controlling the movement at specific middle locations without interacting with neighboring braces, as shown in Fig. 1. Klemperer and Gibbons (1933) analyzed the buckling load of columns with one or two elastic lateral supports, as well as with continuous support using differential equations. Dunn (1941) approximated the buckling load for columns with one or two elastic lateral supports using work-energy methods; Timoshenko (1961) calculated the critical load on a column with continuous elastic support using work-energy methods; and Green (1948) determined the buckling loads of columns with three and four flexible intermediate supports using a work-energy approach with a Fourier series. Green and Winter (1947) proposed an approximate equation for evaluating the axial force-lateral deflection relationships of columns with initial crookedness and verified its accuracy through experiments. Further, Zuk (1956) performed buckling analyses to investigate the axial force generated in point braces while accounting for initial deflection. Winter (1960) initially noted a relationship between the strength and stiffness of point braces.

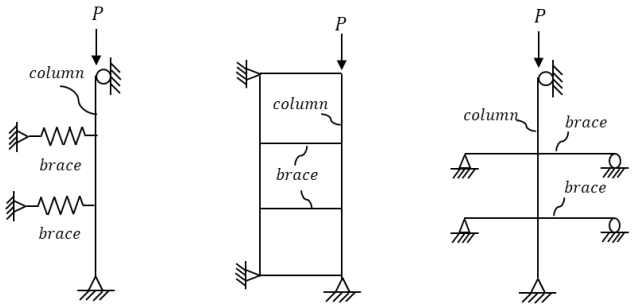

Fig. 1 Intermediate point braces

Lutz and Fisher (1985) outlined stiffness requirements for intermediate-point braces based on a relationship between buckling load and continuous bracing stiffness for continuously braced columns, which considers effective length and column inelasticity. They suggested doubling the ideal stiffness for full bracing to prevent excessive brace force. Building on Winter's findings (1960), Yura (1994) demonstrated that the brace stiffness should be twice the ideal stiffness to prevent excessive axial force in point braces near the buckling load. Plaut and Yang (1993) and

*Corresponding author, Ph.D. Assistant Professor
E-mail: jh.lee@kongju.ac.kr
[a]Ph.D.

ISSN: 1229-9367 (Print), 1598-6233 (Online)

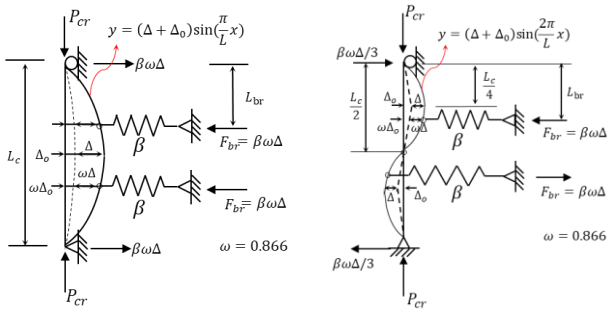

Fig. 2 Free-body diagrams for the buckled shapes of imperfect columns with $n_b = 2$. (a) First, and (b) second buckling modes.

Yura (1995) examined the stiffness and strength of unevenly spaced point braces. The design equations for point braces in the American Institute of Steel Construction (AISC) design specifications (AISC 2022) are based on Yura's strength and stiffness criteria (Yura 1995, Galambos 1998). Gil and Yura (1999) demonstrated through experimental and analytical research that Winter's simplified method for determining the full bracing requirements applies to both inelastic and elastic members. Recent studies (Medland and Segedin 1979, Geng-Shu and Shao-Fan 1987, Zhang *et al*. 2008, Ziemian 2010, Ziemian and Ziemian 2017) investigated the stiffness and strength requirements of point braces for interbraced multicolumn structures. Al-Shawi (Al-Shawi 1998, Al-Shawi 2001) presented an equation for defining the bracing force as a function of the buckling load and bracing stiffness for a single-point brace attached to an arbitrary point on a column under various end conditions. Tran (2009) and Bishop and White (2013) determined the AISC design specification stiffness requirement for point braces to be conservative using a buckling analysis software. Kim and Han (2024) proposed a new procedure to address the limitation of the AISC stiffness equation for end-point braces and Kim *et al*. (2024) suggested new stiffness and strength requirements for intermediate-point braces considering column inelasticity.

Although the strength of single-point braces has been widely studied, no research addressed multiple-point braces because of the lack of a design or analytical equation to determine their strength. Some researchers (AISC 2019, Kim *et al*. 2024) reported that the design of intermediate-point braces in columns with multiple braces is governed by stiffness requirements as per AISC equations rather than by strength requirements. Smaller braces can be used if the strength requirement is increased; further, a factor of two is used in AISC stiffness requirements to limit bracing forces is reduced Kim *et al*. (2024). However, to the best of our knowledge, no studies explored whether more efficient bracing designs can arise when strength requirements, which lead to considerably lower stiffness and higher strength demands, dominate the design. Bracing forces in initially crooked columns under buckling loads are analyzed using analytical methods and compared with finite element analysis (FEA) results to investigate this issue. Based on these findings, practical design requirements and an analytical equation for multiple-point brace strength are proposed.

2. Approximate methods for determining brace forces

The lateral deflection of the column at the point bracing location can be determined by applying Castigliano's theorem to a free-body diagram of the buckling shape of the column when buckling occurs in a column with an initial crookedness (Green 1948). The buckling load (P_{cr}) and bracing force (F_{br}) for the first and second buckling modes of imperfect columns with $n_b = 2$ (Fig. 2) can be defined using Castigliano's theorem via Eqs. (1) and (2), respectively.

$$P_{cr}\left(1 + \frac{\Delta_0}{\Delta}\right) = \left(1 + \frac{5\pi^2\beta}{162}\right) \tag{1a}$$

$$F_{br} = \frac{1}{1500}\frac{\beta P_{cr}}{1 + \frac{5\pi^2\beta}{162} - P_{cr}} \tag{1b}$$

$$P_{cr}\left(1 + \frac{\Delta_0}{\Delta}\right) = \left(4 + \frac{\beta}{12.31}\right) \tag{2a}$$

$$F_{br} = \frac{1}{1500}\frac{\beta P_{cr}}{4.619 + \frac{\beta}{10.661} - \frac{P_{cr}}{0.866}} \tag{2b}$$

$$P_{cr}\left(1 + \frac{\Delta_0}{\Delta}\right) = \left(1 + \frac{\pi^2\beta}{48}\right) \tag{3a}$$

$$F_{br} = \frac{1}{1000}\frac{\beta P_{cr}}{1 + \frac{\pi^2\beta}{48} - P_{cr}} \tag{3b}$$

Sine functions shown in Fig. 2 define the buckling modes of the imperfect columns. In Fig. 2 and Eqs. (1) and (2), L_{br} is $L_c/(n_b+1)$, β represents the stiffness of point braces, and n_b represents the number of point braces. In Eqs. (1) and (2), β and P_{cr} are expressed as fractions of $\frac{P_E}{L_c}$ and P_E, respectively, where P_E represents the Euler elastic buckling load. Similarly, the P_{cr} and F_{br} values of an imperfect column with $n_b = 1$ can be defined by Eq. (3).

Substituting the values of $13.2P_E/L_c$, $81P_E/L_c$, and $16\,P_E/L_c$ corresponding to the buckling mode strengths of $4.973P_E$, $9P_E$, and $4P_E$ for β in Eqs. (1a), (2a), and (3a), respectively, with $\Delta = \infty$, yields buckling loads of $5.02P_E$, $10.58P_E$, and $4.29P_E$. These buckling loads are ~1.23, 17.55, and 7.25 % higher than the target values of $4.973P_E$, $9P_E$, and $4P_E$, respectively. This characteristic causes brace forces to be determined by varying the stiffness of point braces for a given unsafe buckling load. The tendency of Castigliano's theorem to yield unsafe results when buckling shape is defined as a sine function can be improved by defining it as a Fourier series.

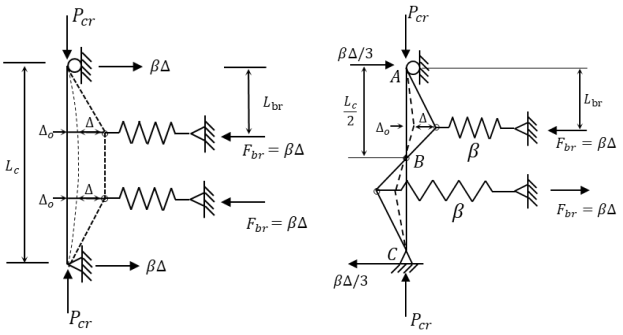

Fig. 3 Winter's rigid-link model for imperfect columns with $n_b = 2$. (a) First, and (b) second buckling modes

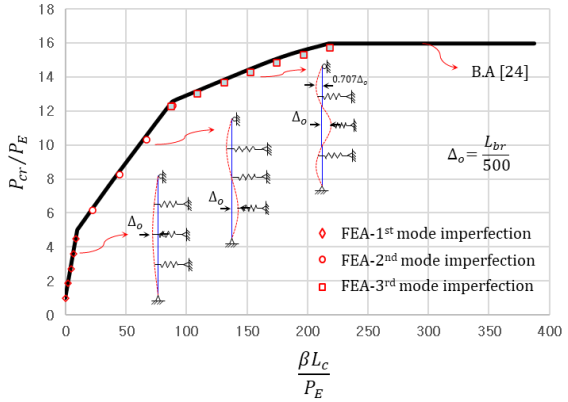

Fig. 4 Comparison of $\beta - P_{cr}$ relationships for perfect and imperfect columns with three-point braces.

Bracing forces for the full (Winter 1960, Yura and Phillips 1992, Yura 1994) and partial bracing strengths (Kim et al. 2024) of columns with initial crookedness can be approximately determined by applying Winter's rigid link model. The P_{cr} and F_{br} can be defined using Eqs. (4) and (5) for the first and second buckling modes of imperfect columns with $n_b = 2$ (Fig. 3) using Winter's rigid-link model. The P_{cr} and F_{br} values for each buckling mode of the imperfect column with any given n_b can be defined by Eq. (6) using Yura's approach. The N_i values for each buckling mode in Eq. (6) are determined via FEA using an initial imperfection shape associated with each buckling mode until the full bracing column strength is achieved. The N_i values are listed in Appendix A.

$$P_{cr}\left(1+\frac{\Delta_0}{\Delta}\right)=\frac{\beta}{3} \tag{4a}$$

$$F_{br}=\frac{1}{1500}\frac{\beta P_{cr}}{\frac{\beta}{3}-P_{cr}} \tag{4b}$$

$$P_{cr}\left(1+\frac{\Delta_0}{\Delta}\right)=\frac{\beta}{9} \tag{5a}$$

$$F_{br}=\frac{1}{1500}\frac{\beta P_{cr}}{\frac{\beta}{9}-P_{cr}} \tag{5b}$$

$$P_{cr}\left(1+\frac{\Delta_0}{\Delta}\right)=\frac{\beta}{N_i(n_b+1)} \tag{6a}$$

$$F_{br}=\frac{1}{500(n_b+1)}\frac{\beta P_{cr}}{\frac{\beta}{N_i(n_b+1)}-P_{cr}} \tag{6b}$$

Fig. 4 shows the $\beta - P_{cr}$ relationships of perfect columns with three-point braces obtained by the buckling analysis (BA) using the energy method with Fourier series (Kim et al. 2024). Fig. 4 also shows the $\beta - P_{cr}$ relationships of imperfect columns with three-point braces obtained using ABAQUS. In the finite element buckling analysis, columns with a length of 48 m and a cross-sectional area of 0.25 m² are modeled using general beam elements (B31 beam elements). The B31 element is a linear beam element with two nodes and six degrees of freedom, suitable for simulating simple beam and column behaviors. Geometrically nonlinear analysis with initial imperfections was conducted to capture the nonlinear column buckling behavior. The column models were assigned a Young's modulus of 205,000 MPa and a Poisson's ratio of 0.3, which represent typical material properties of structural steel. Simply supported boundary conditions were applied, and lateral bending about the strong axis was restrained to focus on the buckling behavior about weak axis bending. The point braces are modeled using spring elements (Spring1) with an elastic axial stiffness of β. For a column model with a slenderness ratio of $\frac{L_c}{r_y} = 332.554$, where r_y represents the radius of gyration about the weak axis, and the mesh refinement indicates that a maximum of 192 beam elements are used. The shapes of the initial imperfections for each buckling mode of the column used in the FEA are presented in Fig. 4. The initial imperfection shape associated with each buckling mode is used for generating the maximum possible bracing force. The zigzag shape of the initial imperfection used for all but the first buckling mode produces the maximum possible bracing force (Winter 1960, Wang and Helwig 2005).

Fig. 4 indicates that the $\frac{\beta L_c}{P_E} - \frac{P_{cr}}{P_E}$ relationships for the column have the same tendency regardless of the presence of initial crookedness. The lateral deflection (Δ) of the crooked column and F_{br} must be infinite to obtain the buckling load (P_{cr}^p) of a perfect column for a given β from a crooked column. The buckling load of a crooked column is zero when Δ is 0 and becomes P_{cr}^p when Δ is ∞. As shown in Eq. (7), the buckling load P_{cr} of a crooked column can be defined as a function of P_{cr}^p and Δ using this relationship. The same equation as Eq. (7) has been proposed by several researchers (Southwell 1932, Green et al. 1947, Yura and Phillips 1992, Yura 1994).

$$P_{cr}\left(1+\frac{\Delta_0}{\Delta}\right)=P_{cr}^p \tag{7}$$

As shown in Fig. 4, the buckling load (P_{cr}^p) of a perfect column for each buckling mode can be approximated as a linear function, as expressed in Eq. (8).

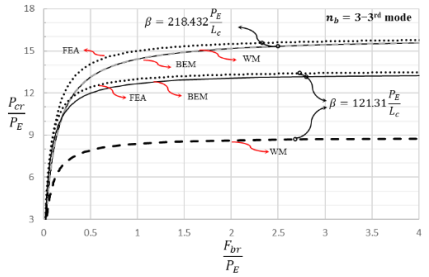

(a)

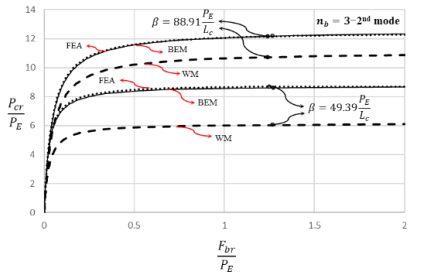

(b)

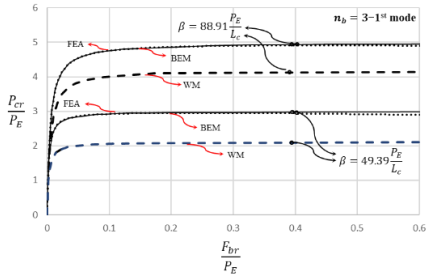

(c)

Fig. 5 Relationships between $\frac{F_{br}}{P_E}$ and $\frac{P_{cr}}{P_E}$ for imperfect columns with $n_b = 3$. (a) Third, (b) second, and (c) first modes.

Further, c_1 and c_2 represent straight-line constants determined from the coordinates of the two points (linearized model). The values of c_1 and c_2 for various buckling modes for n_b=1–5 are listed in Appendix A.

$$P_{cr}^{p} = (c_1 + c_2\beta) \tag{8}$$

The buckling load equivalence model (BEM), which assumes that the buckling load of an imperfect column at infinite lateral deflection matches that of a perfectly straight column, provides reasonable predictions for column-point brace forces. Rearranging Eq. (7) with respect to Δ yields Eq. (9). The F_{br} is defined as the product of the stiffness of point braces and the lateral deflection (Δ) of the column, as indicated in Eq. (10) derived from BEM.

$$\Delta = \frac{P_{cr}}{P_{cr}^{p} - P_{cr}}\Delta_0 = \frac{P_{cr}}{c_1 + c_2\beta - P_{cr}}\Delta_0 \tag{9}$$

$$\begin{aligned} F_{br} = \beta\Delta &= \frac{\beta P_{cr}}{c_1 + c_2\beta - P_{cr}}\Delta_0 \\ &= \frac{\beta P_{cr}}{c_1 + c_2\beta - P_{cr}}\frac{L_c}{500(n_b + 1)} \end{aligned} \tag{10}$$

Fig. 5 shows $\frac{P}{P_E} - \frac{F_{br}}{P_E}$ relationships for the initially crooked columns with $n_b = 3$ obtained using Winter's model (WM) and the BEM along with those determined by FEA. The $\frac{P}{P_E} - \frac{F_{br}}{P_E}$ relationships shown in Fig. 5(a) describe the connection between the axial force (P) and bracing force (F_{br}) by varying the axial force (P) for $\beta = 121.31P_E/L_c$ and $218.432P_E/L_c$. Here, $\beta = 218.432P_E/L_c$ represents the ideal bracing stiffness. The equations for BEM and WM corresponding to this mode are used to determine the $\frac{P}{P_E} - \frac{F_{br}}{P_E}$ relationships because the values of β fall within the range of the third buckling mode. Further, FEA shows that the fastest asymptotic increase to $16P_E$ and $13.51\ P_E$ corresponds to each β. Both WM and BEM are more conservative than FEA, regardless of β. In addition, WM and BEM have the same $\frac{P}{P_E} - \frac{F_{br}}{P_E}$ relationship for ideal bracing stiffness. However, WM was significantly more conservative than BEM when the bracing stiffness was less than the ideal value.

The $\frac{P}{P_E} - \frac{F_{br}}{P_E}$ relationships shown in Fig. 5(b) describe the connection between the axial force (P) and bracing force (F_{br}) obtained by varying the axial force (P) for $\beta = 88.91P_E/L_c$ and $49.39\ P_E/L_c$. The equations for BEM and WM corresponding to this mode were used to determine the $\frac{P}{P_E} - \frac{F_{br}}{P_E}$ relationships because the values of β fall within the range of the second buckling mode. FEA shows the fastest asymptotic increase to $12.2\ P_E$ and $8.57P_E, which$ corresponds to each β. Both WM and BEM are more conservative than FEA regardless of β. The WM is significantly more conservative than the BEM when the bracing stiffness is less than ideal. The $\frac{P}{P_E} - \frac{F_{br}}{P_E}$ relationships obtained by BEM and FEA are closer in the second mode than that in the third mode.

The $\frac{P}{P_E} - \frac{F_{br}}{P_E}$ relationships shown in Fig. 5(c) describe the connection between the axial force (P) and bracing force (F_{br}) obtained by varying the axial force (P) for $\beta = 9.88P_E/L_c$ and $4.94\ P_E/L_c$. The equations for BEM and WM corresponding to this mode were used to determine the $\frac{P}{P_E} - \frac{F_{br}}{P_E}$ relationships because the values of β fall within the range of the first buckling mode. Further, FEA shows the fastest asymptotic increase to $5.0\ P_E$ and $2.88P_E, which$ corresponds to each β. Both WM and BEM are more conservative than that of the FEA, regardless of β. The WM was significantly more conservative than the BEM when the bracing stiffness was less than ideal. The $\frac{P}{P_E} - \frac{F_{br}}{P_E}$ relationships obtained by BEM and FEA were closer in the first mode than that in the second mode.

The BEM and WM are more conservative than that of the FEA, with the WM being particularly conservative for less-than-ideal bracing stiffness. The BEM aligned more closely with the FEA, particularly in the lower buckling modes.

Fig. 6 shows $\frac{\beta L_c}{P_E} - \frac{F_{br}}{P_{cr}^{f}}$ relationships for initially

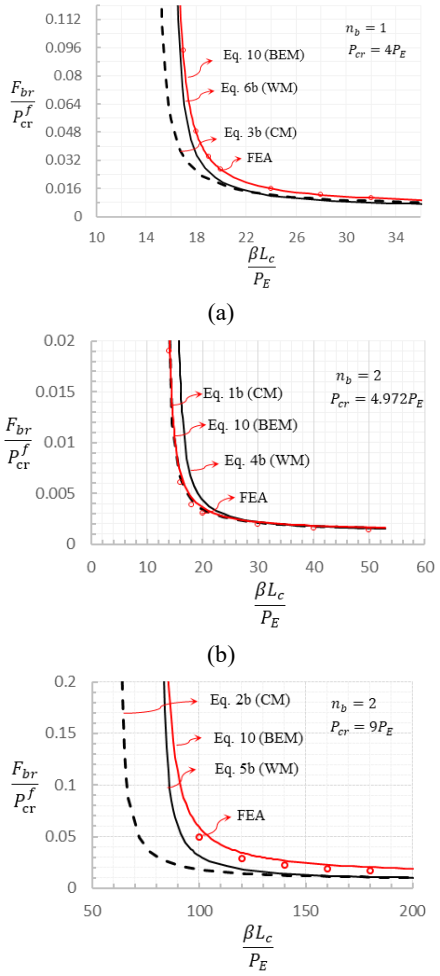

Fig. 6 Relationships between $\frac{\beta L_c}{P_E}$ and $\frac{F_{br}}{P_{cr}^f}$ for imperfect columns. (a) First mode for $n_b = 1$, (b) first mode for $n_b = 2$, and (c) second mode for $n_b = 2$.

crooked columns with $n_b = 1$ and 2 obtained by various approximate methods along with the FEA results. The full bracing column strength P_{cr}^f was expressed as $P_E(n_b + 1)^2$. The relationships $\frac{\beta L_c}{P_E}$ - $\frac{F_{br}}{P_{cr}^f}$ describe the connection between β and F_{br} determined by varying β for a given P_{cr}. The Castigliano model (CM) and WM for full bracing corresponding to the n_b^{th} buckling mode were less conservative than those of the FEA (Figs. 6(a) and 6(c)). The CM requires significantly less β than that of the FEA to achieve the same F_{br} for the full bracing column strength. Although the WM requires more β than that of the CM, it demands considerably less stiffness than that of the FEA. In contrast, the BEM requires a greater β than that of the FEA, which makes it more conservative. For the partial bracing column strength (Fig. 6(b)), the CM, BEM, and WM were more conservative than the FEA, with the CM being the least conservative and the WM the most conservative. For β values exceeding the value at which the F_{br} becomes infinite to achieve the full bracing column strength, the WM and CM produce an unconservative F_{br} at that buckling strength. The BEM is more reasonable than the WM and CM because it is more conservative than FEA, regardless of the buckling load.

3. Brace forces in columns with multiple point braces undergoing elastic buckling

Fig. 7 shows the relationships between $\frac{\beta L_c}{P_E}$ and $\frac{F_{br}}{P_{cr}^f}$ for two buckling loads of initially crooked columns with $n_b = 1, 2,$ and 3 obtained using FEA and the BEM. The mode changes at larger values of the two buckling loads, while the mode remains unchanged at a smaller buckling load. The shape of the initial imperfection for each buckling mode of the column used in both FEA and BEM was identical to that shown in Fig. 4.

Fig. 7(a) shows the relationship between β and F_{br} determined by varying β for the P_{cr} values of $16P_E$ and $14P_E$ for an initially crooked column with $n_b = 3$. In Fig. 7(a), β_{rq}^{16} and β_{rq}^{14} represent brace stiffnesses required to achieve buckling strengths of 16 P_E and 14 P_E, respectively, under the condition that F_{br} becomes infinite. The equations for the BEM corresponding to this mode were used to determine the $\frac{\beta}{P_E} - \frac{F_{br}}{P_{cr}^f}$ relationships because the values of P_{cr} fall within the range of the third buckling mode. Even for a buckling load of $16P_E$, where the buckling mode changed, the BEM equations for the third mode were applied because the buckling mode could not transition to a higher mode without an increase in the buckling load. Buckling strengths of $16P_E$ and $14P_E$ (100 and 87.5 % of the full bracing strength) are developed for initially crooked columns with β values of $2\beta_{rq}^{16}$ and $2\beta_{rq}^{14}$, and the F_{br} values obtained using FEA are $0.0315P_{cr}^f$ and $0.0224\ P_{cr}^f$. These F_{br} values are more than two or three times larger than the expected $0.01P_{cr}^f$, which is calculated by multiplying the β by an amplification factor of two to ensure that these forces are not excessively large (Winter 1960, Lutz and Fisher 1985, Plaut 1993, Plaut and Yang 1993, Yura 1994, Yura 1995, Galambos 1998, AISC 2022). However, F_{br} values obtained using the BEM approach are $0.0381P_{cr}^f$ and $0.0334P_{cr}^f$, which are larger than those determined by the FEA.

Fig. 7(b) shows the relationship between β and F_{br}, as determined by varying the β for P_{cr} values of $9P_E$ and $6P_E$ of an initially crooked column with $n_b = 2$. The values of P_{cr} fall within the range of the second buckling mode, and therefore, the equations for the BEM corresponding to this mode were used for determining the $\frac{\beta}{P_E} - \frac{F_{br}}{P_{cr}^f}$ relationships. For initially crooked columns with β values of $2\beta_{rq}^9$ and $2\beta_{rq}^6$,when buckling strengths of $9P_E$ and $6P_E$ (100 and 67 % of the full bracing strength) are developed. For the full bracing column strength ($9P_E$), F_{br} was greater than $0.01P_{cr}^f$, whereas for ~ 67 % of the full bracing strength, F_{br} was less than $0.01P_{cr}^f$. However, the F_{br} values obtained using the BEM approach

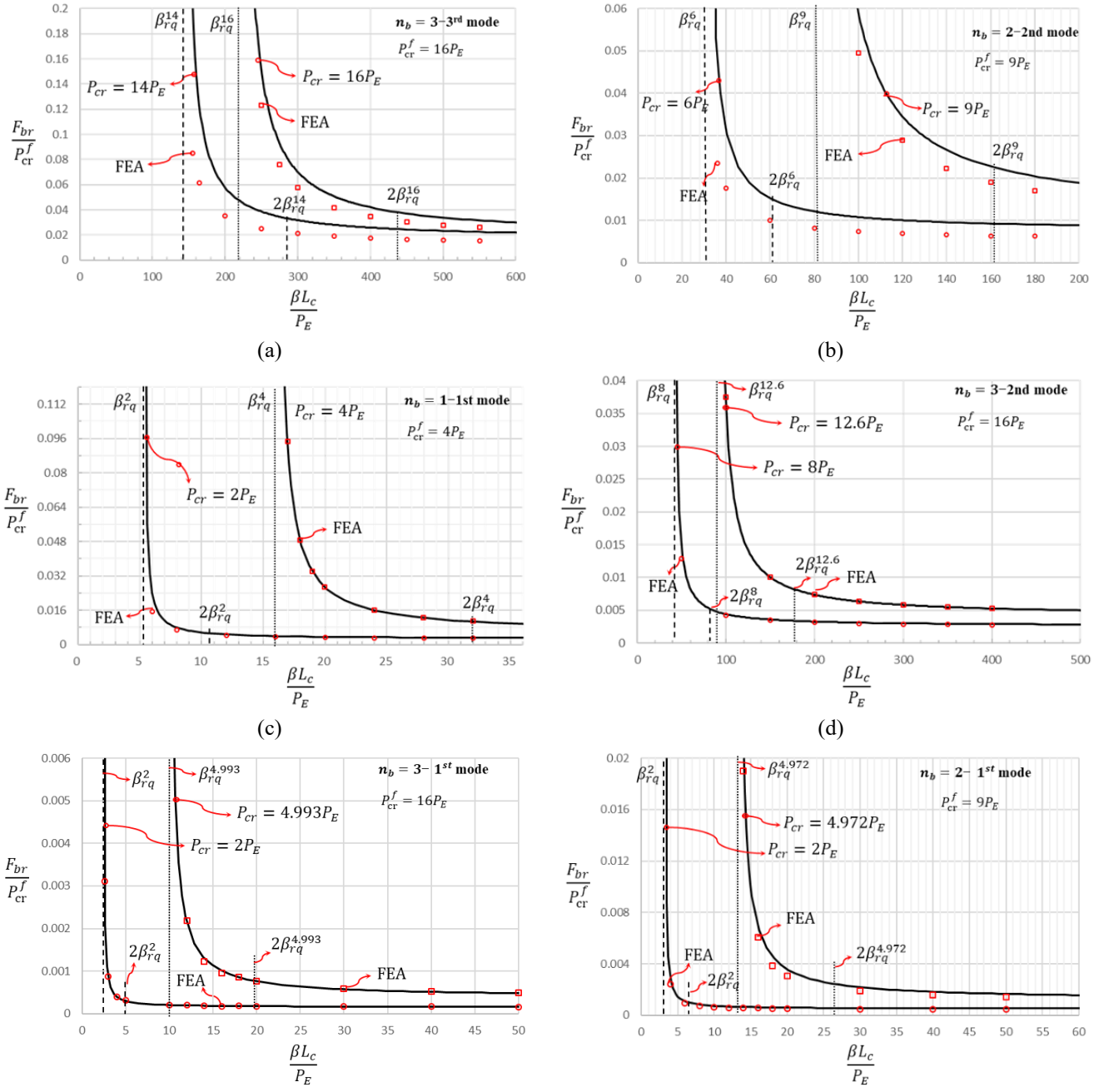

Fig. 7 Relationships between $\frac{\beta L_c}{P_E}$ and $\frac{F_{br}}{P_{cr}^f}$ for imperfect elastic columns. (a) Third mode for $n_b = 3$, (b) second mode for $n_b = 2$, (c) first mode for $n_b = 1$, (d) second mode for $n_b = 3$, (e) first mode for $n_b = 3$, and (f) first mode for $n_b = 2$.

were $0.0224P_{cr}^f$ and $0.0150P_{cr}^f$, which were larger than those determined by the FEA.

Fig. 7(c) shows the relationship between β and F_{br} values determined by varying the β for P_{cr} values of $4P_E$ and $2P_E$ of an initially crooked column with $n_b = 1$. The values of P_{cr} fall within the range of the first buckling mode, and therefore, the equations for the BEM corresponding to this mode are used to determine the $\frac{\beta}{P_E} - \frac{F_{br}}{P_{cr}^f}$ relationships. For initially crooked columns with β values of $2\beta_{rq}^4$ and $2\beta_{rq}^2$, when buckling strengths of $4P_E$ and $2P_E$ (100 and 50 % of the full bracing strength) are developed. For the full bracing strength ($4P_E$), F_{br} was greater than $0.01P_{cr}^f$, whereas for the 50 % full bracing strength, F_{br} was less than $0.01P_{cr}^f$. Meanwhile, the BEM approach yielded almost the same F_{br} values as those determined using FEA.

Fig. 7(d) shows the relationship between β and F_{br} determined by varying β for P_{cr} values of $12.6P_E$ and $8P_E$ of

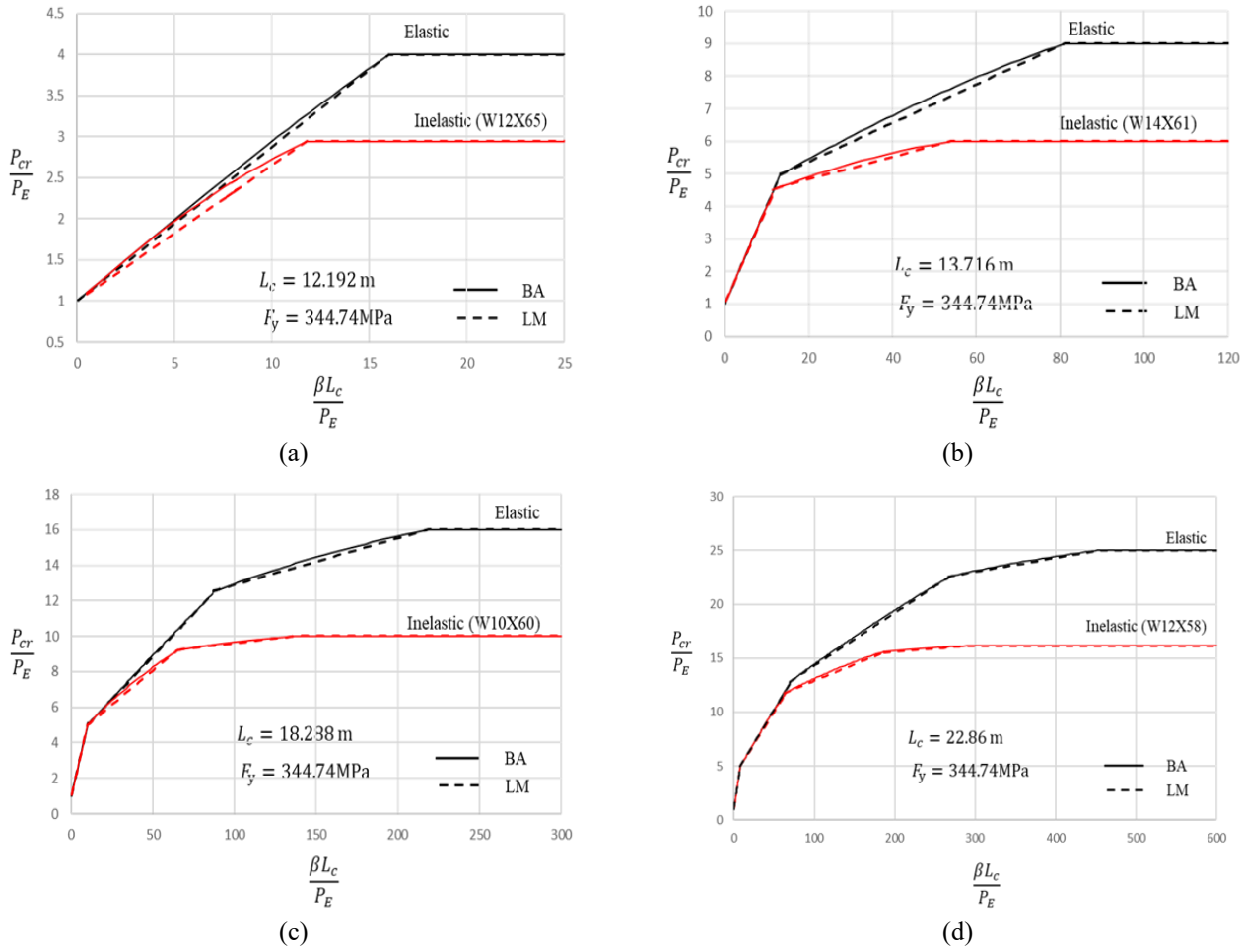

Fig. 8 Relationships between $\frac{\beta L_c}{P_E}$ and $\frac{P_{cr}}{P_E}$ for imperfect columns by BA and LM. (a) n_b=1, (b) $n_b = 2$, (c) $n_b = 3$, and (d) $n_b = 4$.

an initially crooked column with $n_b = 3$. Since the values of P_{cr} fall within the range of the second buckling mode, the equations for the BEM corresponding to this mode were used to determine the $\frac{\beta}{P_E} - \frac{F_{br}}{P_{cr}^f}$ relationships. For initially crooked columns with β values of $2\beta_{rq}^{12.6}$ and $2\beta_{rq}^{8}$, when buckling strengths of $12.6P_E$ and $8P_E$ (79 and 50 % of the full bracing strength) were developed, the F_{br} values obtained using FEA were $0.0082P_{cr}^f$ and $0.0053P_{cr}^f$, both less than $0.01P_{cr}^f$. Practically, the BEM approach produced the same F_{br} values as those in that of the FEA.

Figs. 7(e) and 7(f) show the relationship between β and F_{br} determined by varying the β for P_{cr} values of $4.993P_E$ and $2P_E$ for an initially crooked column with $n_b = 3$, and $4.972P_E$ and $2P_E$ for an initially crooked column with $n_b = 2$. Since the values of P_{cr} fall within the range of the first buckling mode, the equations for the BEM corresponding to this mode were used to determine the $\frac{\beta}{P_E} - \frac{F_{br}}{P_{cr}^f}$ relationships. For initially crooked columns with $n_b = 3$ and β values of $2\beta_{rq}^{4.993}$ and $2\beta_{rq}^{2}$, the F_{br} values obtained using FEA are $0.000762P_{cr}^f$ and $0.000309P_{cr}^f$, which are both less than $0.01P_{cr}^f$, when buckling strengths of $4.993P_E$ and $2P_E$ (31.2 and 12.5 % of the full bracing strength) are developed. Similarly, for $n_b = 2$ and β values of $2\beta_{rq}^{4.972}$ and $2\beta_{rq}^{2}$, when buckling strengths of $4.972P_E$ and $2P_E$ (55.2 and 22.5 % of the full bracing strength) are developed, the F_{br} obtained using FEA are $0.000762P_{cr}^f$ and $0.000309P_{cr}^f$, which are also less than $0.01\,P_{cr}^f$. Practically, the BEM approach produces the same F_{br} values as those in FEA.

Even if the critical β that causes F_{br} to become infinite in achieving the buckling strength of the elastic columns is doubled, the resulting bracing forces for the full or nearly full bracing strength remain significantly greater than that of $0.01P_{cr}^f$. This tendency increased with the number of braces. The BEM predicted slightly greater bracing forces than the FEA for full bracing strengths, where the buckling modes changed, except for $n_b = 1$. This difference is more pronounced for buckling loads below the full bracing strength (associated with the n_b^{th} mode), where the buckling modes do not change, except for $n_b = 1$ because the linearized model (Eq. (8)) underestimates the exact theoretical buckling load for a given β, thereby causing the BEM (Eq. (10)) to predict larger bracing forces.

4. Brace forces in columns with multiple point braces undergoing inelastic buckling

Fig. 8 shows the relationship between $\frac{\beta L_c}{P_E}$ and $\frac{P_{cr}}{P_E}$ for both elastic and inelastic perfect columns with varying numbers of point braces. These relationships were determined using a linearized model (LM; Eq. (8)) of $\beta - P_{cr}$ relationships, as well as the BA employing the energy method and Fourier series (Kim et al. 2024). The LM demonstrated $\frac{\beta L_c}{P_E} - \frac{P_{cr}}{P_E}$ relationships closely matching those obtained from the BA, irrespective of whether the buckling was elastic or inelastic. The linear constants c_1 and c_2 for the buckling load (P_{cr}^p, as defined in Eq. (8)) for a perfect column in each buckling mode should be based on the inelastic coordinates of the start and end points of the mode when using the LM to define the $\beta - P_{cr}$ relationship for columns undergoing inelastic buckling. The inelastic coordinates can be derived using Eq. (11) (Kim et al. 2024), which is formulated from the BA, or by scaling the elastic coordinates of the starting and ending points of each buckling mode by the corresponding stiffness reduction factor τ. The stiffness reduction factor τ can be defined using Eq. (12), which was derived from the ratio of the inelastic buckling stress to the elastic buckling stress, as specified in the AISC design specification. In Eq. (11), i, α, and γ represent the i^{th} buckling mode, $2(n_b + 1)$, and $\alpha - 2 \times i$, respectively. The stiffness reduction factors at the start and end points of each buckling mode can be determined iteratively using Eqs. (13) and (12), respectively, which helps ensure that the assumed P_{cr} is equal to the calculated P_{cr}. In Eq. 13, v_{ep} is a constant that defines the elastic buckling load ($v_{ep}P_E$) at the start and end points of each buckling mode. For a full bracing column, $v_{ep} = (n_b + 1)^2$.

$$\frac{\beta L_c}{P_E} = \frac{\frac{\tau \pi^2}{(n_b+1)}}{\sum_{n=i,\, i+\gamma,\, i+\alpha,\, i+\gamma+\alpha,\, i+2\alpha, i+\gamma+2\alpha,\, i+3\alpha, \cdots}^{\infty} \frac{1}{n^2\left(\frac{P_{cr}}{\tau P_E} - n^2\right)}} \tag{11}$$

$$\tau = 1.0 \;\; if \;\; 0 \le p \le 0.39 \;\; \text{where} \;\; p = \frac{P_{cr}}{P_y} \tag{12a}$$

$$\tau = -2.724\, p(\ln p) \;\; \text{if} \;\; 0.39 < p \le 1.0 \tag{12b}$$

$$P_{cr} = \tau v_{ep} P_E \tag{13}$$

The relationship between the buckling loads of the crooked and perfect columns with identical β values differ between elastic and inelastic buckling. For inelastic buckling, Eq. (8), which defines the relationship for elastic buckling, was modified to Eq. (14). This change reflects the phenomenon in which the ratio of initial crookedness to lateral displacement decreases sharply compared to that with elastic buckling when the yielding progresses. In Eq. (14), $f(\tau)$ represents an empirically determined function of τ. Solving Eq. (14) for Δ results in Eq. (15). The F_{br} is defined by Eq. (16) as the product of β and Eq. (15). In Eq. 16(b), i represents the i^{th} buckling mode.

$$P_{cr}[1 + f(\tau)\frac{\Delta_0}{\Delta}] = P_{cr}^p \tag{14}$$

$$\Delta = \frac{P_{cr}}{P_{cr}^p - P_{cr}} f(\tau)\Delta_0 = \frac{P_{cr}}{c_1 + c_2\beta - P_{cr}} f(\tau)\, \Delta_0 \tag{15}$$

$$\begin{aligned} F_{br} = \beta\Delta &= \frac{\beta P_{cr}}{c_1 + c_2\beta - P_{cr}} f(\tau)\, \Delta_0 \\ &= \frac{\beta P_{cr}}{c_1 + c_2\beta - P_{cr}} \frac{1}{500(n_b+1)} f(\tau) \end{aligned} \tag{16a}$$

$$f(\tau) = 1 \;\; \text{for the first buckling mode}$$

$$f(\tau) = \tau^{\frac{2}{n_b}i - \tau} \frac{1}{\sqrt{(i+0.3)\tau}} \;\; \text{for the other buckling modes} \tag{16b}$$

Fig. 9 shows the relationships between $\frac{\beta L_c}{P_E}$ and $\frac{F_{br}}{\tau P_{cr}^f}$ for two buckling loads of initially crooked inelastic columns with $n_b = 1, 2,$ and 3 obtained using FEA and BEM. For $n_b = 1$ and $n_b = 2$ (Figs. 9(b)-9(d)), the mode changes at larger buckling loads, whereas it remains unchanged at smaller buckling loads. For $n_b = 3$ (Fig. 9(a)), the mode changes at both buckling loads; the larger value corresponds to the full bracing strength, and the smaller value corresponds to the partial bracing strength. The shape of the initial imperfection for each buckling mode of the column used in both FEA and BEM was identical to that shown in Fig. 4. An inelastic buckling analysis using FEA was conducted by performing an elastic buckling analysis with the tangent modulus. The relationship between the point brace stiffness and buckling load for a column undergoing inelastic buckling directly corresponds to that of a column undergoing elastic buckling, which is adjusted by a stiffness reduction factor corresponding to the inelastic buckling load. A critical brace stiffness exists at which the bracing force becomes infinite for a given buckling load associated with a specific stiffness reduction factor. Consequently, if an elastic buckling analysis is performed using FEA with the same tangent modulus and critical brace stiffness, it will yield the target buckling load at which the bracing force becomes infinite. At this target buckling load, an elastic FEA using the same tangent modulus and varying brace stiffness can predict the bracing forces for each brace stiffness identical to those obtained from an inelastic buckling analysis. P_{cr}=5.68P_E

Fig. 9(a) illustrates the relationship between β and F_{br} obtained by varying β for buckling loads P_{cr}=5.68P_E and P_{cr}=5.48P_E of an initially crooked column with $n_b = 3$. The BEM equations for the associated modes were used to determine the $\frac{\beta}{P_E} - \frac{F_{br}}{\tau P_{cr}^f}$ relationships because these P_{cr} values fall within the range of the third and second buckling modes, respectively. For initially crooked columns with β values of $2\beta_{rq}^{5.68}$ and $2\beta_{rq}^{5.48}$, when buckling strengths of 5.68P_E and 5.48P_E (100 and 96.5 % of the full bracing strength) are developed. For the full bracing strength (5.68P_E), F_{br} is more than three times greater than $0.01\tau P_{cr}^f$, while for 96.5 % full bracing strength, F_{br} is less than $0.01\tau P_{cr}^f$. On the other hand, F_{br} values obtained using the

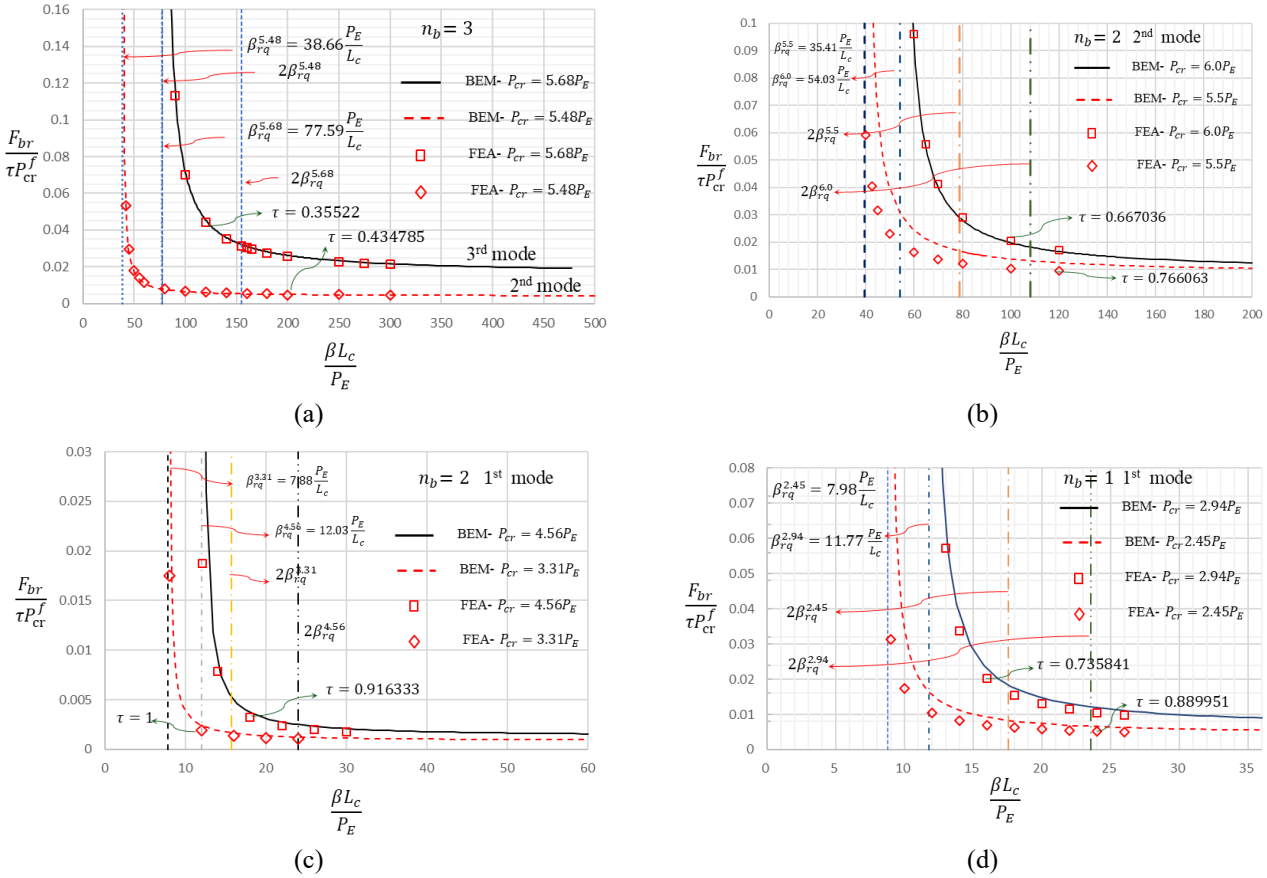

Fig. 9 Relationships between $\frac{\beta L_c}{P_E}$ and $\frac{F_{br}}{\tau P_{cr}^f}$ for the imperfect inelastic columns. (a) Third and second modes for $n_b = 3$, (b) second mode for $n_b = 2$, (c) first mode for $n_b = 2$, and (d) first mode for $n_b = 1$

BEM approach are and $0.0078\ \tau P_{cr}^f$ ($0.0114\ P_{cr}^f$ and $0.0034 P_{cr}^f$) which are larger than those determined by FEA, respectively.

Fig. 9(b) illustrates the relationship between β and F_{br} obtained by varying β for buckling loads P_{cr}=$6.00P_E$ *and* P_{cr}=$5.50P_E$ of an initially crooked column with $n_b = 2$. These P_{cr} values fall within the range of the second buckling mode, and therefore, the equations for the BEM corresponding to this mode were used to determine the $\frac{\beta}{P_E} - \frac{F_{br}}{\tau P_{cr}^f}$ relationships. For initially crooked columns with β values of $2\beta_{rq}^{6.00}$ and $2\beta_{rq}^{5.50}$ the F_{br} values obtained using FEA are $0.0181\ \tau P_{cr}^f$ and $0.0123\ \tau P_{cr}^f$ ($0.0121\ P_{cr}^f$ and $0.0094\ P_{cr}^f$) which are both significantly larger than $0.01\ \tau P_{cr}^f$ when buckling strengths of $6.00P_E$ and $5.50\ P_E$ (100 and 91.7 % of the full bracing strength) are developed. The F_{br} values obtained using the BEM approach are $0.0181\tau P_{cr}^f$ and $0.016\tau P_{cr}^f$ $0.0121\ P_{cr}^f$ and $0.0128 P_{cr}^f$ which are larger than those determined by FEA, respectively.

Fig. 9(c) illustrates the relationship between β and F_{br} obtained by varying β for buckling loads P_{cr}=$4.56P_E$ and P_{cr}=$3.31P_e$ of an initially crooked column with $n_b = 2$. Since these P_{cr} values fall within the range of the first buckling mode, the equations for the BEM corresponding to this mode were used to determine the $\frac{\beta}{P_E} - \frac{F_{br}}{\tau P_{cr}^f}$ relationships. For initially crooked columns with β values of $2\beta_{rq}^{4.56}$ and $2\beta_{rq}^{3.31}$ when buckling strengths of $4.56P_E$ and $3.31P_E$ (75.9 and 55.2 % of the full bracing strength) are developed. F_{br} values obtained using the BEM approach are $0.00250\tau P_{cr}^f$ and $0.00167\ \tau P_{cr}^f$ ($0.00229 P_{cr}^f$ and $0.00167 P_{cr}^f$), which are larger than those determined by that using FEA.

Fig. 9(d) illustrates the relationship between β and F_{br} obtained by varying β for buckling loads P_{cr}=$2.94P_E$ and P_{cr}=$2.45P_e$ of an initially crooked column with n_b=1. Since these P_{cr} values fall within the range of the first buckling mode, the equations for the BEM corresponding to this mode were used to determine the $\frac{\beta}{P_E} - \frac{F_{br}}{\tau P_{cr}^f}$ relationships. For initially crooked columns with β values of $2\beta_{rq}^{2.94}$ and $2\beta_{rq}^{2.45}$ when buckling strengths of $2.94P_E$ and $2.45P_E$ (100 and 83.3 % of the full bracing strength) are developed. For the full bracing strength ($2.94P_E$), F_{br} is larger than $0.01\tau P_{cr}^f$, while for the 83.3 % full bracing strength, F_{br} is less than $0.01\tau P_{cr}^f$. Meanwhile, the F_{br} values obtained using the BEM approach are which are $0.0121\tau P_{cr}^f$ and

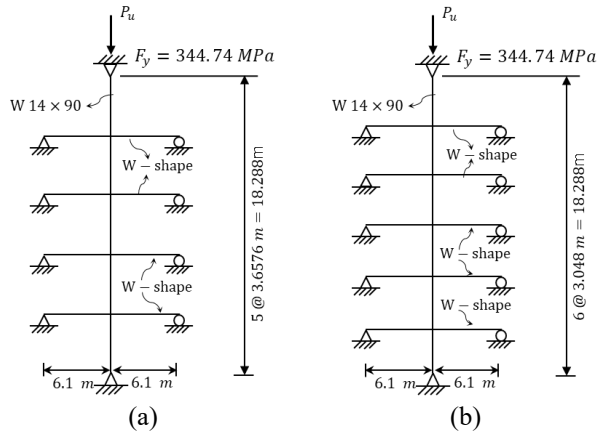

Fig. 10 Point braces for W-shaped columns. (a) Four-point braces, and (b) five-point braces

$0.0083\tau P_{cr}^{f}$ ($0.0089P_{cr}^{f}$ and $0.0074P_{cr}^{f}$), larger than those determined by FEA, respectively.

Even if the critical β that causes F_{br} to become infinite for achieving the buckling strength of inelastic columns is doubled, the resulting F_{br} values for full or nearly full bracing column strength still significantly exceed $0.01\tau P_{cr}^{f}$. Similar to elastic buckling, this tendency increases with the number of braces. Similar to elastic buckling, the BEM approach for inelastic buckling tends to predict slightly higher bracing forces than that of the FEA for buckling loads where the buckling modes change. This disparity becomes even more pronounced for buckling loads without mode changes because the linearized model (Eq. (8)) underestimates the exact theoretical buckling load for a given β, thereby leading to BEM (Eq. (16)) for predicting significantly higher F_{br} values.

5. Design of intermediate point braces for columns

The design of column point braces involves satisfying stiffness requirements for achieving a specific buckling load and ensuring that braces satisfy strength requirements to withstand forces generated by this buckling load. The stiffness requirements are defined using Eq. (11), which describes the exact β- P_{cr} relationships. In this study, a linearized model (Eq. (8)) is used because it facilitates the definition of the β- P_{cr} relationships for each buckling mode, defined by Eq. (11), to establish the stiffness requirements. Eq. (17) provides stiffness requirements based on a linearized model. In Eq. (17), l_{bf} can be selected to be greater than or equal to 1 through trial and error in the bracing design process for ensuring that the smallest possible bracing size is achieved. This parameter serves as an amplification factor for limiting excessive bracing forces. In addition, in Eq. (17), ϕ can be set to 0.75. The strength requirements (P_{br}) from the buckling load equivalence model are the same as F_{br} defined by Eq. (16).

$$\beta = \frac{l_{bf}}{\phi}\frac{P_{cr} - c_1}{c_2} \tag{17}$$

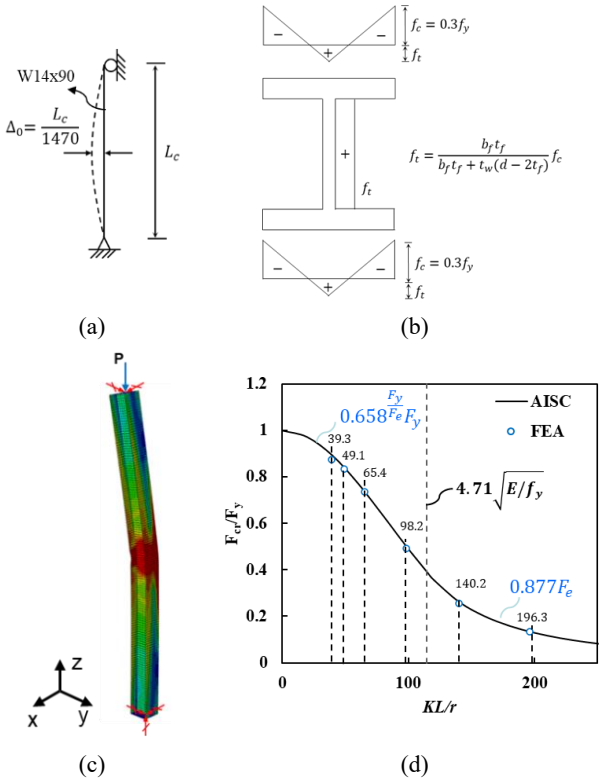

Fig. 11 Comparison of buckling loads from FEA and the AISC column strength curve. (a) Initial imperfection, (b) residual stress pattern (Galambos and Ketter 1959), (c) FEA model, and (d) verification of FEA results with the AISC column strength curve.

A design study was conducted to apply one to five equally spaced point braces to 18.29 m columns undergoing elastic and inelastic buckling. Fig. 10 shows W-shaped columns with four- and five-point braces. All columns had a yield stress of 344.7 MPa, a Young's modulus of 205,000 MPa, and a Poisson's ratio of 0.3. For elastic buckling, the point braces were designed for buckling loads of $4P_E$, $9P_E$, $16\,P_E$, and $25\,P_E$ in the W14 × 90 columns, which correspond to the number of braces. For inelastic buckling, braces were designed for the buckling loads of $3.60P_E$, $5.05\,P_E$, $5.68\,P_E$, and $6.00\,P_E$, thereby matching the maximum inelastic buckling strength of columns with one-to-four-point braces, respectively. The W-shaped beams shown in Fig. 10 served as point braces. The required moment of inertia was calculated by equating the brace stiffness with the ratio of the central load to the vertical deflection of the beam. The required plastic sectional modulus was determined by equating 90 % of the plastic moment to the maximum moment caused by P_{br} (AISC 2019).

Table B-1 in Appendix B presents the stiffness, forces, and member sizes of point braces for elastic columns with one- to five-point braces under various buckling loads. The required brace stiffness and strength for each buckling load decreases with an increase in the number of point braces, regardless of the buckling strength. If availability is not a constraint, increasing the number of braces reduces their member size. The stiffness requirement rises with an

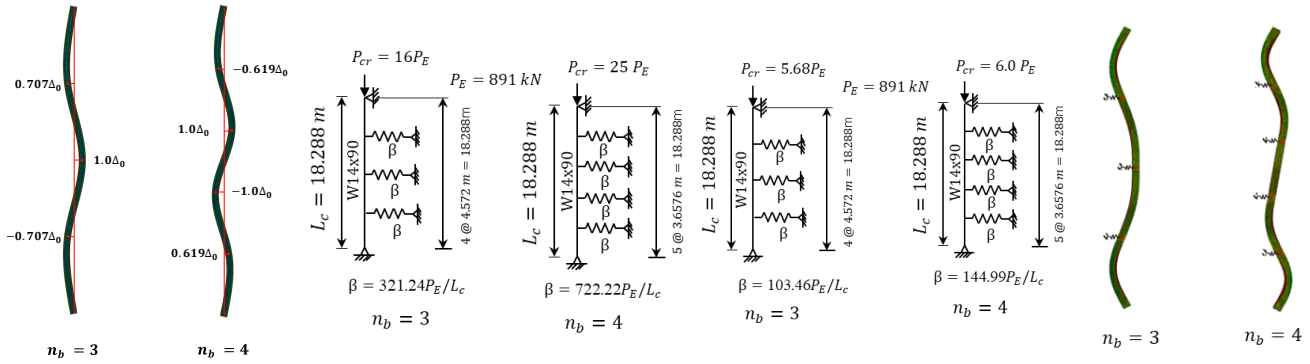

Fig. 12 FEA-modeled columns and their initial and final geometries. (a) Initial imperfections, (b) elastic buckling, (c) inelastic buckling, and (d) final buckled shapes

increase in l_{bf}, while decreasing the strength requirement. The l_{bf} values in Table B-1, which minimize point brace member size, were found to be 1 for all but two buckling loads, with the largest value being 1.196. These values are significantly lower than the commonly used factor of 2, which is intended to prevent large bracing forces. The increase in n_b and P_{cr}^f from 1 and $4P_E$ to 4 and $25P_E$ causes the optimal amplification factor (l_{bf}) which minimizes the weight of a W-shaped cross-section to rise from 1–1.196. In addition, the design shifts from being dominated by stiffness requirements to being governed by strength requirements. The strength requirement P_{br} for fully braced columns with $n_b = 1$ to $n_b = 4$ determined using these l_{bf} values ranges from $0.0213\ P_{cr}^f$ to $0.0823P_{cr}^f$, which is approximately 2.1–8.2 times higher than that of the strength requirement of the AISC of $0.01\ P_{cr}^f$. Although using these optimal l_{bf} values increase the strength requirement, they reduce the stiffness requirement and enables smaller member sizes.

Table B-2 in Appendix B presents similar data for inelastic columns. Similar to elastic columns, the required brace stiffness and strength decrease with an increase in the number of point braces, which reduces the member size when availability is not constrained. For inelastic columns, increasing l_{bf} raises the stiffness requirement and decreases the strength requirement. The l_{bf} values in Table B-2, which minimize the point brace member size, were 1 for all buckling loads, regardless of the number of braces.

These values are half of the commonly used factor of 2. The increase in n_b and τP_{cr}^f, from 1 and $3.6P_E$ to 4 and $6.0P_E$ does not alter the optimal amplification factor (l_{bf}) of 1, which minimizes the weight of a W-shaped cross-section. However, the design shifts from being dominated by stiffness requirements to being governed by strength requirements. The strength requirement P_{br} for fully braced columns with $n_b = 1$ to $n_b = 4$, determined using these l_{bf} values, ranges from $0.0221\tau P_{cr}^f$ to $0.0791\tau P_{cr}^f$, approximately 2.2–7.9 times higher than the requirement of the AISC.

The required brace stiffness β (or the second moment of inertia I_{req}) increases linearly with a steep slope (Eq. (17)) with an increase in l_{bf}, while bracing forces (Eq. (16)) decrease nonlinearly. For $l_{bf} \geq 1$ ($l_{bf}/\phi = 1.33$), the bracing force (or required plastic section modulus Z_{req}) decreases nearly linearly with a gentle slope. At $l_{bf} = 1$, the combination of the smallest I and moderately low Z resulted in a balance between the stiffness and strength requirements, which supports its use as an optimal value for efficient bracing design.

For W-shaped sections, increasing the weight per unit length results in a simultaneous increase in I and Z. However, I_{req} increases as with an increase in l_{bf}, while Z_{req} decreases, creating opposing trends. In the range $0.75 < l_{bf} < t_{cf}$ ($1 < l_{bf}/\phi < 1.33t_{cf}$), the weight per unit length of the lightest W-shaped section that satisfies both Z_{req} and I_{req} decreases with an increase in l_{bf} because the strength requirement (Z_{req}) governs the design. For $l_{bf} \geq t_{cf}$ ($l_{bf}/\phi \geq 1.33t_{cf}$), the weight per unit length of the lightest section increases with an increase in l_{bf} because the stiffness requirement (I_{req}) becomes dominant. The transition coefficient t_{cf} is typically defined as 1; however, it can increase substantially beyond 1 as both n_b and P_{cr}^f increase significantly, particularly in elastic buckling. The dominant state of the bracing design transitioned from strength to stiffness when $l_{bf} = t_{cf}$.

Applying a fixed l_{bf} value of 1 to the bracing design for inelastic buckling produces brace member sizes equivalent to those determined by optimally varying l_{bf}, which identifies the smallest brace sizes. Although it can lead to slightly larger brace sizes for certain buckling loads, using a fixed l_{bf} value of 1 increases computational efficiency. However, this approach produces the smallest brace size. Smaller member sizes for point braces and more efficient designs were achieved across all buckling loads by applying an optimal varying l_{bf}, which allows strength to exceed AISC specification values and stiffness to fall below them for elastic and inelastic buckling (or $l_{bf} = 1$ for inelastic buckling), to linearized stiffness requirements from Eq. (17) and the strength requirement from Eqs. (16), which reasonably predict the bracing forces. This approach is

Table 1 Comparison of bracing forces from FEA and the buckling load equivalence model

Type	n_b	τP_{cr}^f	$\frac{\beta L_c}{P_E}$	$\left(\frac{P_{br}}{P_E}\right)_{BEM.}$	$\left(\frac{P_{br}}{\tau P_{cr}^f}\right)_{BEM.}$	$\left(\frac{P_{br}}{P_E}\right)_{FEA}$	$\left(\frac{P_{br}}{\tau P_{cr}^f}\right)_{FEA.}$	Difference (%)
Elastic buckling	3	$16P_E$	321.24 (147.1 %)	0.9528	0.0595	1.199	0.075	−20.5
	4	$25P_E$	722.22 (159.5 %)	2.0573	0.0823	1.575	0.063	30.6
Inelastic buckling	3	$5.68P_E$	103.46 (133.3 %)	0.3283	0.0578	0.103	0.018	218.7
	4	$6.0P_E$	144.99 (133.3 %)	0.4746	0.0791	0.052	0.009	812.7

Table 2 Bracing forces from beam-element FEA and shell-element FEA

Type	n_b	τP_{cr}^f		Beam-element FEA				Shell-element FEA			
			τ	$\left(\frac{P_{br}}{P_E}\right)_{FEA}$	$\left(\frac{P_{br}}{\tau P_{cr}^f}\right)_{FEA.}$	Difference (%)	$\left(\frac{P_{br}}{P_E}\right)_{FEA}$	$\left(\frac{P_{br}}{\tau P_{cr}^f}\right)_{FEA.}$	Difference (%)	
Elastic buckling	3	$16P_E$	1	1.046	0.065	−8.9	1.046	0.065	−8.9	
	4	$25P_E$	1	1.003	0.04	105.1	1.733	0.069	18.7	
Inelastic buckling	3	$5.68P_E$	τ_a	0.35522	0.471	0.083	-30.3	0.128	0.023	156.5
			τ_b	0.48396	0.132	0.023	148.7			
	4	$6.0P_E$	τ_a	0.24011	0.146	0.024	225.1	0.123	0.021	285.9
			τ_b	0.336	0.090	0.015	427.3			

more efficient than the AISC method, where a fixed l_{bf} of the two results in unnecessarily high stiffness and low strength requirements. The linearized stiffness and proposed strength requirements, whether using a fixed $l_{bf} = 1$ or an optimally varying l_{bf}, lead to a lower bracing stiffness, higher strength, and smaller member size for point braces, which optimizes both stiffness and strength.

FEA was performed on the columns shown in Fig. 10 with $n_b = 3$ and $n_b = 4$ to validate the bracing design for columns with point braces. The FEA models are calibrated by comparing the buckling loads obtained through the FEA with AISC column strength curves, as shown in Fig. 11.

The initial imperfections and residual stress distributions for columns with slenderness ratios ranging from 39.3–196.3, as shown in Fig. 11, are incorporated into the FEA. Flanges and webs are modeled as shell elements (S4R elements) to consider both geometrical and material nonlinearities, and residual stresses. Through mesh refinement, the number of analytical elements increased from 640 to 3184 with an increase in the slenderness ratio from 39.3 to 196.3 with a constant mesh size of 46 × 46 mm used across all models. The load and boundary conditions of the FEA models were same as those provided in Section 2. In addition, the point braces were modeled using spring elements (Spring) with an elastic axial stiffness of β. These spring elements were attached to the designated brace points, and each brace point was connected to the web section using the multi-point constraints (MPC) option provided in the ABAQUS program. The ratio of buckling loads from the FEA to those from the AISC column strength curves for six different configurations was found to range from 0.972 to 0.999, which confirms that the FEA closely aligns with the AISC column strength curves.

Among the bracing designs in Tables B-1 and B-2 in Appendix B, those for the full bracing of columns with $n_b = 3$ and $n_b = 4$ subjected to elastic and inelastic buckling were selected for FEA verification, as shown in Fig. 12. The residual-stress distribution and initial imperfections applied to FEA models are shown in Figs. 11(b) and 12(a), respectively. The initial imperfections in Fig. 12(a) represent the zigzag-type third and fourth eigenmodes for columns with $n_b = 3$ and $n_b = 4$, which are expected to produce the largest bracing forces. The point braces were modeled using spring elements for minimizing the restraint of column deformation, thereby enabling the maximum possible bracing force to occur. A multipoint constraint (MPC) option was applied to the cross-section at the installation location to mitigate stress concentrations in the column web caused by spring element installation. Table 1 compares bracing forces determined from the FEA with the strength requirements of the buckling load equivalence model for point braces.

For braces with $n_b = 3$ and $n_b = 4$ subjected to elastic buckling, bracing forces determined by FEA were respectively −20.5 and 30.6 % smaller than those calculated using the strength requirements from BEM. For inelastic buckling, the discrepancies were significantly larger, with the FEA-determined bracing forces being 218.7 and 812.7

% smaller at $n_b = 3$ and $n_b = 4$, respectively. These results indicate that differences between FEA and BEM predictions increase with an increasing n_b in elastic buckling and are further magnified in inelastic buckling. A negative percentage difference indicated that FEA predicted a higher bracing force than that of the BEM. However, the difference was not sufficiently significant to exceed the margin provided by the safety factor.

In inelastic buckling, the bracing force predicted by FEA was substantially smaller than that predicted by the BEM because the bracing stiffness in inelastic buckling is closer to the critical stiffness (refer to the numbers in parentheses in the $\beta L_c/P_E$-related column of Table 1). Near the critical stiffness, the relationship between bracing stiffness and bracing force becomes highly nonlinear (see Figs. 7 and 9), thereby causing small changes in the stiffness and resulting in substantial differences in bracing forces. Consequently, the bracing stiffness required by FEA and BEM to produce the same bracing force in this region differs significantly, and this can lead to pronounced differences in bracing forces predicted by FEA and BEM when the stiffness is held constant.

Inelastic buckling analyses (Beam-Element FEA) using the tangent modulus, similar to the inelastic analysis in Section 4, were conducted using two types of stiffness reduction factors τ_a and τ_b to further investigate the bracing forces determined by FEA and BEM in inelastic buckling. Further, the analyses incorporated the initial deformation pattern shown in Fig. 12(a) and utilized beam elements. Further, inelastic buckling analyses (shell element FEA) were performed to consider the residual stress distribution shown in Fig. 11(b). These analyses utilized shell elements and accounted for a combined initial deformation, which incorporates modes from the first to the n_b^{th} mode. This deformation comprises zig-zag patterns similar to those in Fig. 12(a) and a half-sine curve with an amplitude of $\Delta_0 =$ L/1470 shown in Fig. 11(a). The stiffness reduction factor τ_a defined by Eq. 12 was used for calibrating the BEM. In contrast, τ_b, which is a higher stiffness reduction factor determined using the CRC column curve was defined as $\tau = 4\,p(1-p)$ for $p > 0.5$ and $\tau = 1$ for $p \leq 0.5$.

Table 2 compares bracing forces determined from the shell element and beam element FEA. Since the BEM was calibrated to beam-element FEA with τ_a, the difference between beam-element FEA with τ_a and BEM is smaller than the difference between beam-element FEA with τ_b and BEM. The beam-element FEA with τ_a, which accounts for the effect of the initial deformation and reflects the progression of column yielding more rapidly, produced greater bracing forces than that of the beam-element FEA with τ_b.

The shell-element FEA, which incorporates a combined initial imperfection, predicts higher bracing forces than the shell-element FEA with only zigzag deformation, except in the case of elastic buckling for $n_b = 3$. However, for inelastic buckling at $n_b = 3$, it yields smaller bracing forces compared to that of the beam-element FEA with τ_b. This outcome can be attributed to the fact that the shell-element FEA tends to predict smaller bracing forces than that of beam-element FEA with τ_b because yielding is concentrated at locations where the zig-zag pattern is prominent, thereby causing the target buckling load to be reached without the significant lateral displacement of the column. These analyses indicate that the shape of the initial deformation has a significant effect on the magnitude of the bracing forces.

These findings indicate that the shape of the initial deformation significantly affects the magnitude of the predicted bracing forces, particularly under inelastic buckling, where localized yielding can dominate. BEM produced the largest bracing force among the analyzed methods; however, BEM is limited in accurately defining bracing forces for multiple-point braces because it relies on the simplified assumption that the buckling load of a column with an initial imperfection at an infinite lateral displacement is equivalent to that of a perfectly straight column. This assumption does not account for the complex effects of elastic and inelastic buckling, which includes the sensitivity to initial imperfections and the progression of yielding. Although a lower strength requirement is unlikely to affect the size of the bracing member as the stiffness requirement dominates the design, more accurate bracing forces can be obtained by calibrating BEM with the shell-element FEA or beam-element FEA with τ_b. Such a calibration allows the BEM to better reflect the actual behavior of braces under these conditions, thereby providing a more precise basis for design decisions.

6. Conclusions

For the economical design of column braces, by achieving a balance between stiffness and strength requirements of the column bracing systems, this study investigated the improved strength requirements for multiple-point braces in column members, which has remained insufficiently addressed due to the lack of appropriate design or analytical equations. To enable practical and rational design approaches, a rational brace strength design method for multiple-point braces is proposed. A summary of this study is provided below.

• This study proposed BEM method to establish the relationships between the buckling load and the corresponding bracing forces. Based on the relationships between $\frac{F_{br}}{P_E}$ and $\frac{P_{cr}}{P_E}$ obtained from the BEM, the bracing forces of the multiple-point braces in columns were evaluated and compared with the results from the Castigliano method (CM), winter method (WM) and finite element analysis (FEA) results.

• By comparing the bracing forces obtained from the BEM and other analytical approaches, it was found that the BEM requires greater bracing stiffness than the FEA, making it more conservative. In contrast, the WM and CM tend to yield non-conservative bracing forces under full bracing conditions. For partial bracing, the CM, BEM, and WM provide more conservative results than the FEA, with the CM being the least conservative and the WM the most conservative.

• Even when critical bracing stiffness, which causes the

bracing force to become infinite to reach a target buckling load, is doubled, the forces calculated by FEA for full or nearly full bracing still significantly exceed 1% of the full bracing column strength ($0.01P_{cr}^{f}$), which is the basis of bracing design provision specified in AISC design specification, for elastic buckling of columns. This trend intensifies with an increase in the number of braces. Similar trends were also observed during the inelastic buckling of columns with multiple-point braces.

• The BEM approach for both elastic and inelastic buckling tends to predict slightly higher bracing forces than those obtained from the FEA, particularly at buckling loads associated with mode changes. This disparity becomes more pronounced at buckling loads without mode changes because the linearized model underestimates the exact theoretical buckling load for a given β, thereby leading to BEM for predicting significantly higher F_{br} values.

• Applying an optimal varying amplification factor that enables the strength to exceed the AISC specification values and stiffness to fall below them to the linearized stiffness and strength requirements from the buckling load equivalence model leads to smaller member sizes and more efficient designs. This method outperforms the AISC approach, in which a fixed amplification factor of two results in excessively high stiffness and unnecessarily low strength requirements. The proposed approach effectively reduces bracing stiffness, increases strength, and optimizes member sizes for point braces, thereby achieving a more balanced and economical design.

Acknowledgments

This work was supported by DS Global ECM Co., Ltd. and supported by the research grant of Kongju National University Industry-University cooperation foundation in 2025.

References

AISC (2019), *Companion to the AISC Seel Cnstruction Mnual, Vol. 1: Design Examples, Version 15.1*, American Institute of Steel Construction, Chicago, IL.

AISC (2022), *Specification for Structural Steel Buildings*, American Institute of Steel Construction, Inc., Chicago, IL.

Al-Shawi, F.A.N. (1998), "Etermination of restraint forces for steel struts", *Proc Inst Civ Eng Struct Build*., **128,** 282-289.

Al-Shawi, F.A.N. (2001), "Stiffness of restraint for steel struts with elastic end supports", *Proc Inst Civ Eng Struct Build*. **146**(2), 153-159.

Bishop, C.D. and White, D.W. (2013), "Practical design of complex stability bracing configurations", *Proceedings of the Annual Stability Conference Structural Stability Research Council*, St. Louis, Missouri, April.

Dunn, C.A. (1941), *A Study of Columns having Elastic Lateral Supports*, Cornell University

Galambos, T.V. (1998), *Guide to Stability Design Criteria for Metal Structures,* John Wiley & Sons, New Jersey.

Galambos, T.V. and Ketter, R.L. (1959), "Columns under combined bending and thrust", *J. Eng. Mech. Div.*, **85**(EM2), 135-152.

Geng-Shu, T. and Shao-Fan, C. (1987), "Design forces of horizontal inter-column braces", *J. Constr. Steel Res.*, **7** 363-370.

Gil, H. and Yura, J.A. (1999), "Bracing requirements of inelastic columns", *J. Constr. Steel Res.*, **51**, 1-19.

Green, G.G. (1948), *Lateral Buckling of Elastically Braced Columns*, Cornell University

Green, G.G., Winter, G. and Cuykendall, T.R. (1947), *Light Gage Steel Columns in Wall-braced Panels*, Cornell University, New York.

Hawileh, R.A., Abed, F., Abu-Obeidah, A.S. and Abdalla, J.A. (2012), "Experimental investigation of inelastic buckling of built-up steel columns", *Steel Compos. Struct*., **13**(3), 295-308.

Juk, W. (1956), "Lateral bracing forces on beams and columns", *J. Eng. Mech. Div.*, **82** 1032-1031 - 1032-1016.

Kemperer, W.B. and Gibbons, H.B. (1933), "Über die Knickfestigkeit eines auf elastischen Zwischenstützen gelagerten Balkens", *ZAMM-Journal of Applied Mathematics and Mechanics/Zeitschrift für Angewandte Mathematik und Mechanik*. **13** 251-259.

Kim, K.D. and Han, K.J. (2024), "Design method for determining appropriate stiffness for end point braces", *J. Constr. Steel Res.*, **212**.

Kim, K.D., Park, K.Y., Choi, Y.G. and Kong, B.J. (2024), "Intermediate-point bracing for columns: New stiffness–buckling load formulae", *J. Constr. Steel Res.*, **222**, 108967.

Leblouba, M., Barakat, S., Awad, R., AI-Khaled, S.U., Metawa, A. and Karzad, A.S. (2024), "buckling behavior of bundled inclined columns: Experimental study and design code verification", *Steel Compos. Struct*., **52**(2), 183-197.

Lee, D.-S. (2004), "Inelastic distortional buckling of hot-rolled I-section beam-columns", *Steel Compos. Struct*., **4**(1), 23-36.

Lee, J., Byun, N., Kang, Y.J., Won, D.H. and Kim, S. (2022), "Axial compression behavior of double-skinned composite tubular columns under pure compression on concrete cores", *Steel Compos. Struct*., **43**(4), 431-445.

Lutz, L.A. and Fisher, J.M. (1985), "A unified approach for stability bracing requirements", *Eng. J., AISC*. **22**(4), 163-167.

Medland, I.C. and Segedin, C.M. (1979), "Brace forces in interbraced column structures", *J. Struct. Div.*, **105**, 1543-1556.

Plaut, R.H. (1993), "Requirements for lateral bracing of columns with two spans", *J. Struct. Eng.*, **119**, 2913-2931.

Plaut, R.H. and Yang, J.G. (1993), "Lateral bracing forces in columns with two unequal spans", *J. Struct. Eng.*, **119**, 2896-2912.

Seo, J., Won, D. and Kim, S. (2022), "Comparative study between inelastic compressive buckling analysis and Eurocode 3 for rectangular steel columns under elevated temperatures", *Steel Compos. Struct*., **43**(3), 341-351.

Dassault Systèmes (2020), *Abaqus 2020 Documentation. Providence*, RI, USA: Dassault Systèmes Simulia Corp.

Southwell, R.V. (1932), "On the analysis of experimental observations in problems of elastic stability", *Proc. Roy. SOC. (London), Series A*. **135**, 601.

Timoshenko, S.P. (1961), *Theory of Elastic Stability,* McGraw-Hill, New York.

Tran, D.Q. (2009), *Towards Improved Flange Bracing Requirements for Metal Building Frame Systems*, Georgia Institute of Technology

Wang, L. and Helwig, T.A. (2005), "Critical imperfections for beam bracing systems", *J. Struct. Eng.*, **131**(6), 933-940.

Winter, G. (1960), "Lateral bracing of columns and beams", *Trans. Am. Soc. Civ. Eng.*, **125**, 807-826.

Yura, J.A. (1994), "Winters Bracing Model Revisited", *50th Anniv. Proc. SSRC*. 375-382.

Yura, J.A. (1995), "Bracing for stability—State-of-the-art", *In Restructuring: America and Beyond, ASCE*. 88-103.

Yura, J.A. and Phillips, B. (1992), *Bracing Requirements for*

Elastic Steel Beams, Report No. 1239-1, Center for Transportation Research, University of Texas at Austin

Zhang, Y., Zhao, J. and Zhang, W. (2008), "Parametric studies on inter-column brace forces", *Adv. Struct. Eng.*, **11**, 293-303.

Ziemian, R.D. (2010), *Guide to Stability Design Criteria for Metal Structures,* John Wiley & Sons, New Jersey.

Ziemian, R.D. and Ziemian, C.W. (2017), "Formulation and validation of minimum brace stiffness for systems of compression members", *J. Constr. Steel Res.*, **129,** 263-275.

CC

Appendix A

Table A-1 Constants for the linearized and Winter models for $n_b = 1$ to 5

n_b	Mode	Linearized model		Winter model	
		c_1	c_2	N_i	$N_i \cdot (n_b+1)$
1	First	1.000	0.188	2	4
2	First	1.000	0.301	1.000	3.000
	Second	4.189	0.059	3	9.000
3	First	1.000	0.404	0.586	2.344
	Second	4.042	0.096	2.000	8.000
	Third	10.269	0.026	3.413	13.652
4	First	1.000	0.506	0.380	1.898
	Second	4.016	0.124	1.374	6.868
	Third	9.413	0.049	2.602	13.010
	Fourth	19.097	0.013	3.623	18.116
5	First	1.000	0.608	0.266	1.594
	Second	4.006	0.151	0.991	5.947
	Third	9.147	0.065	1.982	11.894
	Fourth	17.623	0.029	2.974	17.841
	Fifth	30.254	0.007	3.731	22.388

Appendix B

Table B-1 Stiffness and strength of point braces for elastic columns

$n_b = 5$ ($P_E = 891.0\ kN$; $P_{cr}^f = 36P_E$)								
P_u	Buckling mode	$\frac{\beta L_c}{P_E}$	$\frac{l_{bf}\beta L_c}{\phi P_E}$	$\frac{F_{br}}{P_{cr}^f}$	$\frac{I_{req}}{cm^4}$	$\frac{Z_{req}}{cm^3}$	Brace member	l_{bf}
$4P_E$	1	4.94	6.58	0.0002	6056	77	W14X22	1.000
$9P_E$	2	33.06	44.08	0.0022	40554	695	W21X50	1.000
$16P_E$	3	106.14	141.51	0.0092	130188	2892	W30X90	1.000
$25P_E$	4	254.55	339.40	0.0320	312239	10068	W36X160	1.000
$n_b = 4$ ($P_E = 891.0\ kN$; $P_{cr}^f = 25P_E$)								
P_u	Buckling mode	$\frac{\beta L_c}{P_E}$	$\frac{l_{bf}\beta L_c}{\phi P_E}$	$\frac{F_{br}}{P_{cr}^f}$	$\frac{I_{req}}{cm^4}$	$\frac{Z_{req}}{cm^3}$	Brace member	l_{bf}
$4P_E$	1	5.93	7.90	0.0005	7272	111	W14X22	1.000
$9P_E$	2	40.06	53.42	0.0046	49141	1013	W24X55	1.000
$16P_E$	3	134.42	179.23	0.0209	164883	4573	W30X99	1.000
$25P_E$	4	452.90	722.22	0.0823	664416	18008	W44X230	1.196
$n_b = 3$ ($P_E = 891.0\ kN$; $P_{cr}^f = 16P_E$)								
P_u	Buckling mode	$\frac{\beta L_c}{P_E}$	$\frac{l_{bf}\beta L_c}{\phi P_E}$	$\frac{F_{br}}{P_{cr}^f}$	$\frac{I_{req}}{cm^4}$	$\frac{Z_{req}}{cm^3}$	Brace member	l_{bf}
$4P_E$	1	7.42	9.89	0.0012	9101	173	W16X26	1.000
$9P_E$	2	51.50	68.66	0.0117	63165	1637	W24X62	1.000
$16P_E$	3	218.43	321.24	0.0595	295526	8340	W36X135	1.103
$n_b = 2$ ($P_E = 891.0\ kN$; $P_{cr}^f = 9P_E$)								
P_u	Buckling mode	$\frac{\beta L_c}{P_E}$	$\frac{l_{bf}\beta L_c}{\phi P_E}$	$\frac{F_{br}}{P_{cr}^f}$	$\frac{I_{req}}{cm^4}$	$\frac{Z_{req}}{cm^3}$	Brace member	l_{bf}
$4P_E$	1	9.96	13.28	0.0039	12216	310	W16X26	1.000
$9P_E$	2	81.00	108.00	0.0449	99356	3537	W27X84	1.000
$n_b = 1$ ($P_E = 891.0\ kN$; $P_{cr}^f = 4P_E$)								
P_u	Buckling mode	$\frac{\beta L_c}{P_E}$	$\frac{l_{bf}\beta L_c}{\phi P_E}$	$\frac{F_{br}}{P_{cr}^f}$	$\frac{I_{req}}{cm^4}$	$\frac{Z_{req}}{cm^3}$	Brace member	l_{bf}
$4P_E$	1	16.00	21.33	0.0213	19626	747	W18X35	1.000